Structure, Optical, Magnetic and Photocatalytic Properties of Cu doped $ZnFe_2O_4$ Nanoparticles

Kunpeng GE [1], Xiaoyi CHENG [1], Junchao QIAN [1], Chengbao LIU [1], Feng CHEN [1, 2] *

[1] *School of Materials Science and Engineering, Suzhou University of Science and Technology, Suzhou, 215009, China*
[2] *Jiangsu Key Laboratory for Environment Functional Materials, Suzhou University of Science and Technology, Suzhou, 215009, China*

http://doi.org/10.5755/j02.ms.41304

Received 28 April 2025; accepted 6 June 2025

Copper doped zinc ferrite (Cu-$ZnFe_2O_4$) nanocrystallites were synthesised via the sol-gel process. X-ray diffraction (XRD), Field Emission Scanning Electron Microscopy (FE-SEM), UV–visible spectroscopy, and Vibrating Sample Magnetometry (VSM) were utilised to analyse the structural behaviour and magnetic properties of the sample. X-ray diffraction studies revealed the spinel FCC structure of the sample. The scanning electron microscopy micrographs indicated the formation of crystallites with dense, compact and platelet structure. The absorption spectrum and the Tauc plot revealed the bandgap to be 2.0 eV. The sample's magnetic property was analyzed using a vibrating sample magnetometer, confirming its superparamagnetic behaviour at room temperature. The photocatalytic degradation of the sample was assessed against Methylene Blue (MB) dye in visible light irradiation, demonstrating an efficiency of 83%. The elemental composition of the sample and its oxidation state were determined using X-ray photoelectron spectroscopy (XPS), which confirmed the synthesis of Cu-doped $ZnFe_2O_4$.
Keywords: Cu doped zinc ferrite, nanostructure, magnetic property, XPS, photocatalytic activity, nanoparticles.

1. INTRODUCTION

Ferrites are ceramic-like materials with unique magnetic properties that are used in many electronic devices. Spinel-structured ferrites are the important materials employed in contemporary engineering, both in scientific and practical applications [1]. Ferrites have high magnetic permeability, high electrical resistance, high coercivity and so on. Magnetic ceramics are classified as hard (hexaferrites) and soft (spinels and garnets) magnetic materials [2, 3]. In recent decades, spinel soft ferrites have garnered significant attention. Spinels are ascribed with general chemical formula AB_2O_4, which crystallize in cubic structure with thermal stability, making them suitable for various applications. These materials are utilized in microelectronics, magnetic memory, gas sensors, water purifiers, catalysis, biomedical, antimicrobial and magnetic resonance imaging applications [4]. Among the ferrites, zinc ferrite ($ZnFe_2O_4$) is an outstanding material, suitable for several applications [5]. $ZnFe_2O_4$ possesses significant applications in several domains, including sensors, energy, photocatalysis, spintronics and information storage. The performance of this material is critically dependent on its inherent features. The incorporation of different metal ions, including magnetic and nonmagnetic ions into the spinel structure alters the physical and chemical properties [6, 7]. The distribution of cations is contingent upon the ionic radii of cation, synthesis method, preparation parameters, doping, sintering temperature, and substitution process. These results in unique electric and magnetic characteristics for specific applications. The doping of copper (Cu) in zinc ferrites leads to structural modification and change in properties, optimizing their performance for certain applications. Moreover, it is interesting to note that Cu-doped $ZnFe_2O_4$ nanoparticles offer promising properties. Their performance is highly dependent on the precise control of synthesis parameters and doping concentrations. Ongoing research continues to optimize these factors to fully harness their potential in various applications [8, 9]. Cu-doped $ZnFe_2O_4$ nanoparticles belong to a category of spinel ferrite nanoparticles, which attracted considerable interest due to their improved catalytic properties and prospective applications in magnetic data storage, wastewater treatment, and biomedicine [10 – 13].

Prithviraj Swamy et al. prepared nano crystalline zinc ferrite using the low-temperature combustion method and their XRD results showed single-phase ferrite NPs with a crystallite size of 40 nm [4]. Komal Yadav prepared the Cu doped zinc ferrites using green synthesis route. XRD studies of the samples showed crystalline nature with a crystallite size of 9 nm [14]. Nadhiya et al synthesized $Cu_xZn_{(1-x)}Fe_2O_4$ NPs using sol-gel process and studied the structure and magnetic properties [15]. Vani et al. synthesized the copper doped zinc ferrite NPs and studied the structure and optical properties [16]. Bera et al. prepared the zinc ferrite and the XRD and XPS were used to study the ferrite NPs [17]. The synthesis method and preparation conditions significantly influence the properties of ferrite NPs for their intended uses in the present context. Numerous strategies have been documented for the preparation of nanomaterials, including precipitation, high-energy ball milling, hydrothermal methods, combustion routes, solvothermal methods, microwave-assisted synthesis, thermal plasma, micro-emulsion techniques and sol-gel processes [18, 19].

* Corresponding author: F. Chen
E-mail: *chenfeng@mail.usts.edu.cn*

In the present work, Cu doped zinc ferrite nanoparticles have been synthesized using sol-gel technique due to its simplicity, cleanliness, low cost and eco-friendliness. This study focuses on the synthesis and characterization of Cu doped zinc ferrite NPs for magnetic and photocatalytic applications.

2. EXPERIMENTAL DETAILS

The analytical reagent (AR) grade compounds were utilized in this study without additional processing. The experiment employed deionized (DI) water consistently. Iron nitrate nonahydrate ($Fe(NO_3)_3{\cdot}9H_2O$) and zinc acetate dihydrate ($Zn(CH_3COO)_2{\cdot}2(H_2O)$) were individually dissolved in deionised water. Both solutions were mixed and agitated for 10 min. Copper nitrate was subsequently dissolved in deionized water and incorporated into the preceding solution for a doping of 10 %. Subsequently, CTAB was incorporated as a surfactant. The citric acid served as the gelling agent. The solution was maintained at around 70 – 80 °C and calcined at 600 °C for 2 h.

X-ray diffraction studies were carried out for the sample Cu doped $ZnFe_2O_4$ using powder diffractometer (BRUKER D8) with CuKα radiation in the range of 20 – 80°. The surface morphology and composition were analyzed using FESEM (CARL ZEISS). The sample's optical characteristics were examined using UV-visible spectrophotometer (Shimadzu) in the 200 – 1000 nm wavelength range. The sample's magnetic characteristics were examined with a vibrating sample magnetometer (LAKESHORE, Model 7407). A 10 ppm MB dye solution was used to assess the sample's degradation performance. The solution was kept under dark condition for 30 min to attain equilibrium and the visible light source (550 nm and 125 W) was used to find the degradation of MB dye solution for 120 min duration. 2 ml of the solution was removed for every thirty minutes while it was exposed to visible light (550 nm). The UV-Vis spectrophotometer was employed to examine the absorbance the sample. The XPS spectra were acquired with a Versa Probe II (ULVAC-PHI, Chigasaki, Japan).

3. RESULTS AND DISCUSSION

3.1. Microstructure analysis

The XRD pattern (Fig.1) shows prominent intensity peaks at angles 18.3°, 30.0°, 35.35°, 36.3°, 42.9°, 47.6°, 53.3°, and 56.7°, which correspond to (111), (220), (311), (222), (400), (331), (422), and (333) reflecting planes, respectively, indicating the single phase spinel fcc structure of $ZnFe_2O_4$, (JCPDS No. 22-1012) [20,21]. In addition, there are peaks at angles 31.8°, and 38.8° correspond to (-110) and (111) planes, indicating the monoclinic structure of CuO. The crystallite size was calculated using the Scherrer formula from the prominent peak (311):

$$D = \frac{K\lambda}{ß\cos\theta}, \quad (1)$$

where K is the Scherrer constant (0.9); λ is the wavelength of X-ray; β is the width at half maximum (FWHM) in radian; θ is the diffraction angle. The crystallite size was found to be 23 nm. Arthur Charles et al. synthesized zinc copper ferrite nanostructures using co-precipitation. XRD studies confirmed the cubic spinel structure of the samples and the crystallite size was found to be 32 nm [22]. Komal et al. [14] prepared copper doped zinc ferrite nanoparticles using green synthesis. The prepared samples showed a crystalline nature with a crystallite size of 9 – 21 nm range. Shwetambaram et al synthesized Cu doped zinc ferrite ($Zn_{(1-x)}Cu_xFe_2O_4$) NPs by the hydrothermal method, and the XRD studies confirmed single phase spinel cubic structure [23].

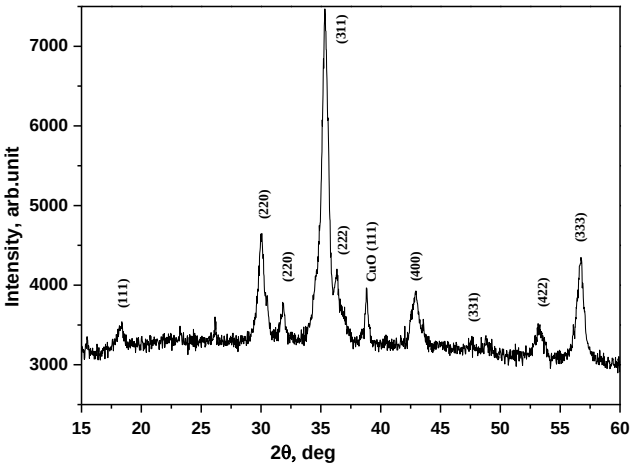


Fig. 1. XRD pattern of Cu doped $ZnFe_2O_4$ nanoparticles

The surface morphology of the NPs was analyzed using FE-SEM. Fig. 2 shows the formation of crystallites with irregular shapes and sizes. It shows the dense structure, smooth morphology with agglomerations. Each grain is constituted by the aggregation of many nanocrystallites. The EDX analysis verified the presence of Zn, Cu, Fe, and O elements in the sample, with no further contaminants detected. This signifies the effective incorporation of Cu into the $ZnFe_2O_4$ matrix. The samples exhibit uneven forms and sizes, with grain cohesion resulting from magnetic attraction [22, 24].

3.2. Optical properties - UV-visible spectroscopy

The absorption spectrum of the Cu-doped $ZnFe_2O_4$ nanoparticles is shown in Fig. 3. The bandgap (E_g) was calculated using absorption phenomena associated with the valence-conduction band transition. A noticeable absorption was observed at about 800 nm, signifying the band-to-band transition. The bandgap (E_g) is determined by the Tauc plot, a plot of $(\alpha h\nu)^2$ versus hν at α=0. (Fig. 3). Eq. 2 is employed to determine the bandgap of the sample.

$$(\alpha h\nu)^2 = A(h\nu - E_g), \quad (2)$$

where α is the absorption coefficient, ν is the frequency of radiation. The bandgap of the sample was found to be 2.0 eV. Vani et al., determined the bandgap of pure $ZnFe_2O_4$ nanoparticles and copper doped nanoparticles. The bandgap was observed to be increasing for higher Cu content in the zinc ferrite system, increasing from 1.825 to 2.776 eV [16].

Ramamurthi et al studied the optical property of the NPs and the bandgap was found to be ~3.05 eV and ~3.51 eV for $ZnFe_2O_4$ NPs prepared using polyethylene glycol (PEG) and cetyltrimethylammonium bromide

(CTAB) capping agents, respectively [24]. The present result is in agreement with the earlier reported values.

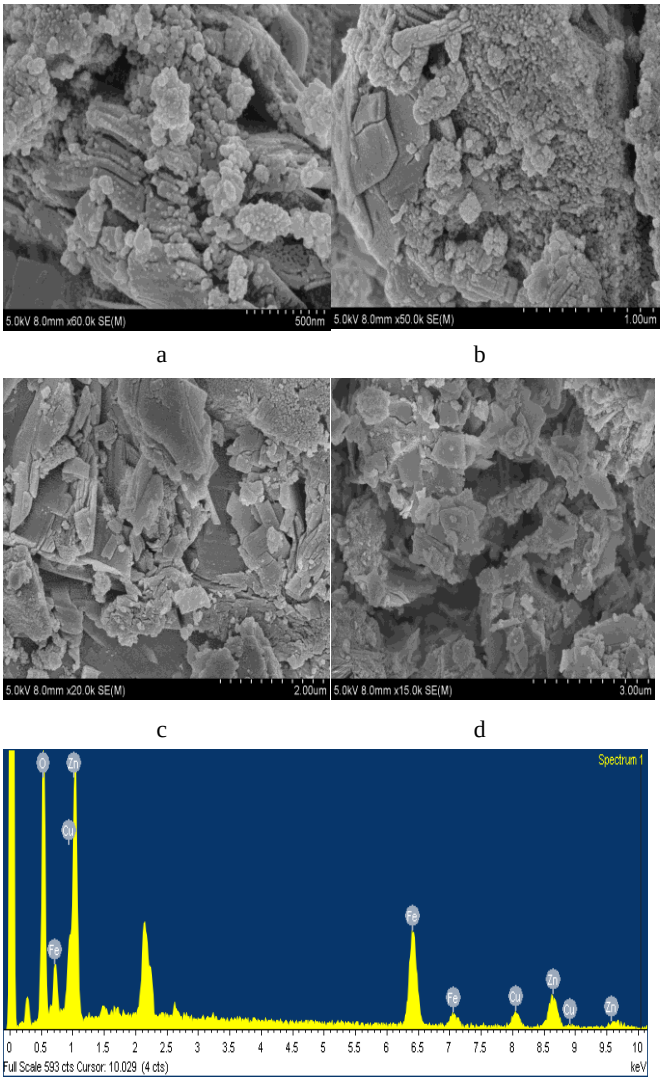


Fig. 2. a – 60 KX; b – 50 KX; c – 20 KX; d – 15 KX; e – EDX analysis of Cu doped $ZnFe_2O_4$ nanoparticles

3.3. Magnetic properties – vibrating sample magnetometer (VSM)

The magnetization behaviour of the Cu-doped $ZnFe_2O_4$ compound was assessed in relation to an applied magnetic field ranging from 0 to 1.5 T. The obtained magnetization curve is shown in Fig. 4, which provides crucial insights into the material's magnetic characteristics. The coercivity (Hc) and retentivity (Mr) values obtained from the magnetization loops, are 19.40 Oe and 0.125×10^{-6} emu, respectively. The M-H curve reveals that the compound possesses a minimal retentivity of 0.125×10^{-6} emu, signifying its feeble remanent magnetization following the removal of the external magnetic field. The dependency of coercivity on crystallite size is well-documented, with smaller crystallite sizes often leading to a transition from multidomain to single domain regimes or superparamagnetic states [25].

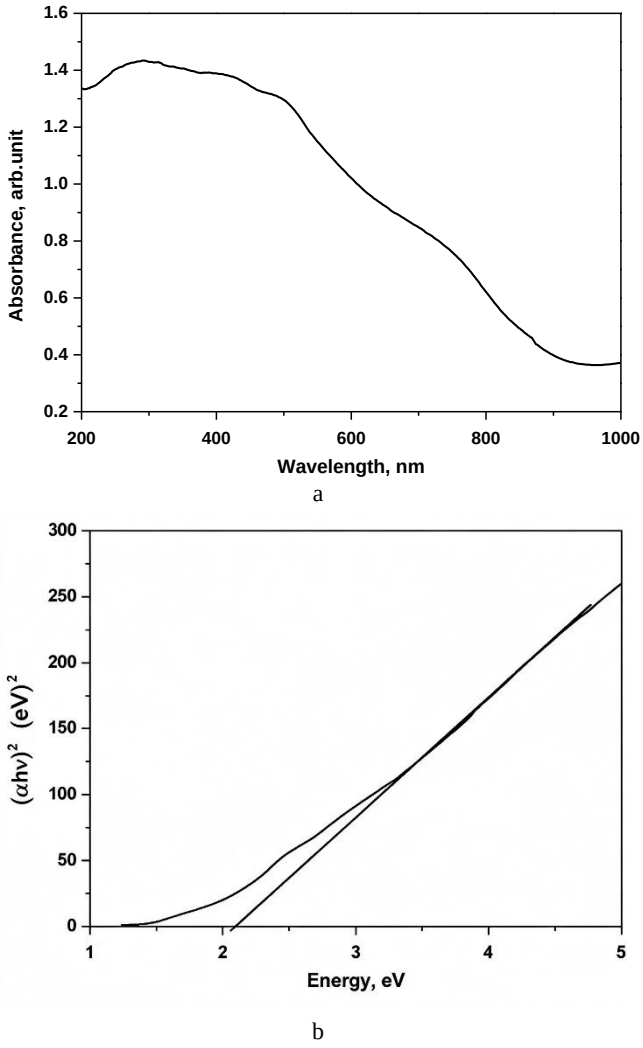


Fig. 3. UV–visible spectroscopy analysis of Cu doped $ZnFe_2O_4$ nanoparticles: a – absorption spectrum; b – Tauc plot

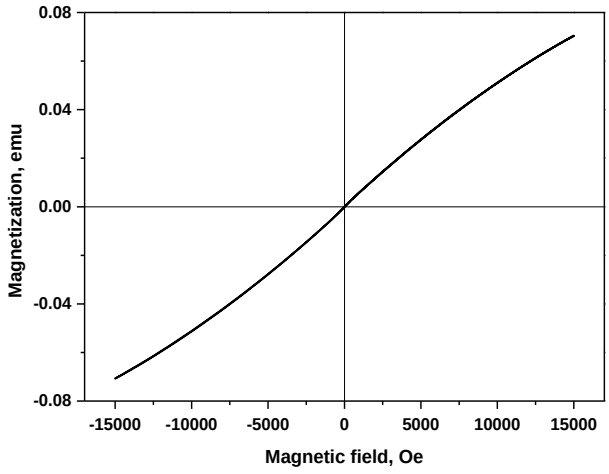


Fig. 4. Magnetic hysteresis loop of Cu doped $ZnFe_2O_4$ nanoparticles

Furthermore, the M−H curve reveals a non-saturation magnetization nature even at the maximum applied magnetic field strength 15,000 Oe. The observed near linear variation in magnetization with increasing magnetic field suggests that the magnetic interactions in the sample are significantly influenced by the doping of non-magnetic Cu^{2+}

ions. This doping disrupts the magnetic ordering of the $ZnFe_2O_4$ spinel structure by substituting Cu^{2+} ions at the octahedral sites traditionally occupied by Zn^{2+} or Fe^{3+}. The introduction of Cu^{2+} ions not only alters the distribution of magnetic ions but also weakens the super exchange interactions between tetrahedral and octahedral sites [26].

The reduced coercivity and lack of magnetic saturation further indicate the material's transition from a superparamagnetic to paramagnetic state. This transition arises due to the reduced magnetic coupling and spin canting effects caused by the presence of Cu^{2+} ions, which have a lower magnetic moment compared to Fe^{3+}. The reduced magnetic moment of Cu^{2+} (1 μB) compared to Fe^{3+} (5 μB) significantly impacts the net magnetization of the compound. Hence, the magnetization studies demonstrate that the Cu doped $ZnFe_2O_4$ compound undergoes a superparamagnetic-to-paramagnetic transition due to the doping of non-magnetic Cu^{2+} ions, which disrupts the intrinsic ferrimagnetic ordering of $ZnFe_2O_4$ compound. This transition and the accompanying magnetic properties can be attributed to changes in crystallite size, spin interactions, and cation distribution within the spinel structure [27]. Arthur Charles et al. synthesized zinc copper ferrite NPs by co-precipitation process and studied the magnetic properties. The results clearly indicated the superparamagnetic behaviour of the sample [20]. zinc ferrite quantum dot (QD) is produced using microwave assisted hydrothermal synthesis and observed dual magnetic behaviour (superparamagnetism/perfect paramagnetism) [28].

3.4. Photocatalytic studies

The photodegradation of MB dye of copper doped zinc ferrite NPs is assessed. The photocatalytic efficiency of the nanoparticles is evaluated over a period of time against MB dye. The characteristic peak about 664 nm diminishes progressively with prolonged exposure from 0 to 2 h. This signifies that the MB dye has been nearly decomposed after 2 h. The performance of zinc copper ferrite has been recorded as 83 % dye degradation due to its capacity to absorb visible light and diminish the electron-hole recombination rate [29 – 31]. Arthur Charles et al. investigated the photocatalytic efficacy of MB dye using visible light, revealing a 65 % efficiency with zinc copper ferrite nanoparticles [18]. Wahid et al. synthesized Cu doped $ZnFe_2O_4$ using a hydrothermal method for MB degradation under visible light radiation and found the degradation efficiency of 97.06 % for $Cu_{0.75}Zn_{0.25}Fe_2O_4$ [29].

3.5. X-ray photoelectron spectroscopy (XPS) studies

XPS spectrum is shown in Fig. 5, which illustrates the presence of Zn, Fe, Cu, and O elements in the sample.

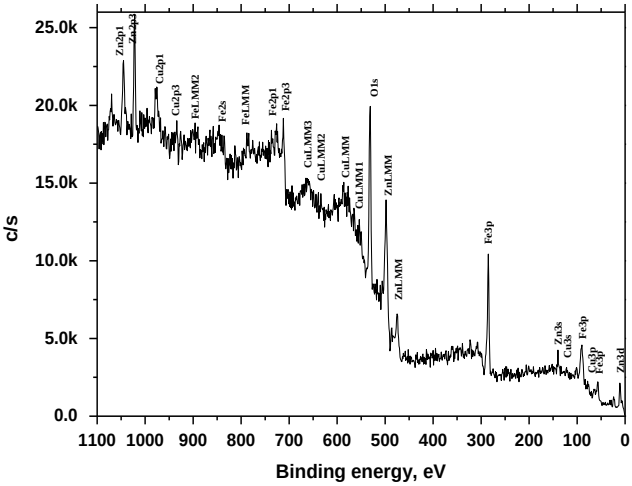
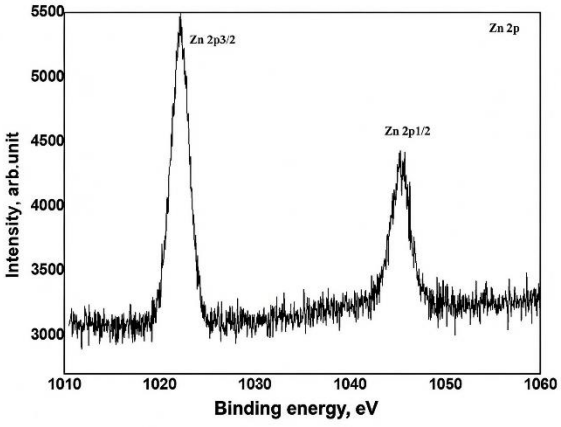
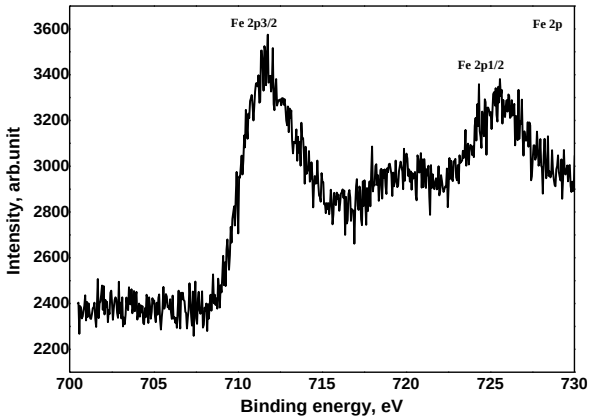


Fig. 5. XPS spectrum shows the peaks of all the elements

The Zn2p spectrum display peaks at 1022 eV and 1045 eV, denoted $Zn2p_{3/2}$ and $Zn2p_{1/2}$, respectively (Fig. 6 a). The peak at 1022 eV is attributed to the Zn^{+2} state, with the zinc atom residing in a tetrahedral location. Fe2p photoelectron spectrum for Cu doped zinc ferrite is shown. The XPS spectrum for $Fe2p_{3/2}$ and $Fe2p_{1/2}$ is shown in Fig. 6 b with peaks at 711 eV and 725 eV, respectively. The binding energy for $Fe2p_{3/2}$ in magnetite is 711 eV, aligning closely with the literature value [27]. The Cu2p spectrum indicates the existence of peaks about 933 and 953 eV denote $Cu2p_{3/2}$ and Cu $2p_{1/2}$, respectively (Fig. 6 c). The peak at 530 eV in the O1s spectra (Fig. 6 d) is attributed to the characteristic lattice oxygen in the Fe–O or Cu–O structure.

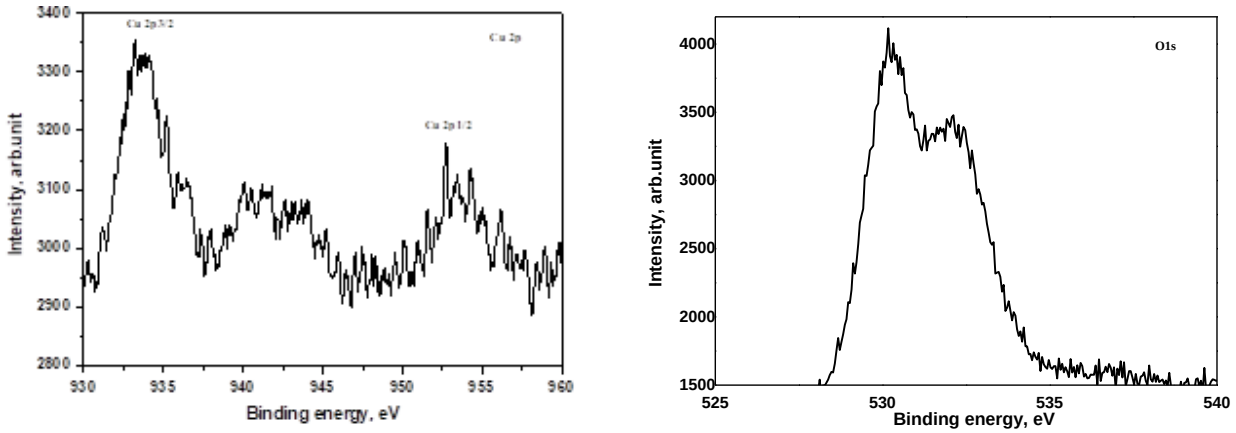


a



b

continued on the next page



c d

Fig. 6. XPS analysis for Cu doped $ZnFe_2O_4$ nanoparticles: a – Zn 2p; b – Fe 2p; c – Cu 2p; d – O 1s

The signal at 530 eV signifies the presence of oxygen from other components adsorbed on the sample's surface. The peak ~532 eV arises from the deficiency of low oxygen coordination in the nanostructure. The peak positions and peak widths agreed with the other reported results [5].

4. CONCLUSIONS

Cu doped $ZnFe_2O_4$ nanoparticles were prepared via the sol-gel technique and subsequently calcined at 600 °C for 2 h. The XRD examination indicated the presence of mixed phases of $ZnFe_2O_4$ and CuO in the synthesized sample. The XRD pattern of the sample showed the peaks indicating the spinel face-centered cubic (FCC) structure with a crystallite size of 23 nm. FE-SEM images showed the prepared nanoparticles exhibiting agglomeration, while the EDX spectrum verifies the presence of Zn, Fe, Cu, and O in the synthesized nanoparticles. VSM measurements indicated that the synthesized ferrites are soft ferrites having superparamagnetic behaviour at room temperature. The synthesised NPs showed effective photocatalytic degradation of MB dye, and the degradation efficiency was 83 % using visible light irradiation. XPS studies revealed the oxidation states of the components in the ferrite sample.

REFERENCES

1. **Dehghani Dastjerdi, O., Shokrollahi, H., Mirshekari, S.** A Review of Synthesis, Characterization and Magnetic Properties of Soft Spinel Ferrites *Inorganic Chemistry Communications* 153 2023: pp. 11079. https://doi.org/10.1016/j.inoche.2023.110797
2. **Fan, G., Gu, Z., Yang, L., Li, F.** Nanocrystalline Zinc Ferrite Photocatalysts formed using the Colloid mill and Hydrothermal Technique *Chemical Engineering Journal* 155 2009: pp. 534 – 541. https://doi.org/10.1016/j.cej.2009.08.008
3. **Qiu, J., Wang, C., Gu, M.** Photocatalytic Properties and Optical Absorption of Zinc Ferrite Nanometer Films *Materials Science and Engineering: B* 112 2004: pp. 1 – 4. https://doi.org/10.1016/j.mseb.2004.04.012
4. **Prithviraj Swamy, P.M., Basavaraja, S., Arunkumar, L., Srinivas Rao, N.V., Nijagunappa, R., Venkataraman, A.** Synthesis and Characterization of Zinc Ferrite Nanoparticles obtained by Self-propagating Low-Temperature Combustion Method *Bulletin of Materials Science* 34 2011: pp. 1325 – 1330. https://doi.org/10.1007/s12034-011-0323-x
5. **Kumar, P., Mathpal, M.C., Inwati, G.K., Kumar, S., Duvenhage, M.M., Roos, W.D., Swart, H.C.** Study of Defect Induced Chemical Modifications in Spinel Zinc Ferrites Nanostructures by In-Depth XPS Investigation *Magnetochemistry 9* 2023: pp. 20. https://doi.org/10.3390/magnetochemistry9010020
6. **Saha, P., Rakshit, R., Alam, M., Mandal, K.** Magnetic and Electronic Properties of Zn Doped Fe_3O_4 Hollow Nanospheres *Physical Review Applied* 11 2019: pp. 024059. https://doi.org/10.1016/j.jmmm.2018.11.061
7. **Shanmugam, A.K., Rathanasamy, R., Kaliyannan, G.V., Nagarajan, N., Palanisamy, M.** Spinel Zinc Ferrite Nanostructured Thin-films for Enhanced light-Harvesting in Polycrystalline Solar Cells *Materials Science-Poland* 39 2021: pp. 24 – 32. https://doi.org/10.2478/msp-2021-0002
8. **Kuru, T.Ş., Kuru, M.** Structural, Optical, and Dielectric Properties of Cu, Ni-doped Zn Ferrites *Journal of the Australian Ceramic Society* 55 2019: pp. 781 – 788. https://doi.org/10.1007/S41779-018-00290-7
9. **Muhammad, Z., Hasan, M.K., Muhammad, Z.M., Hafiz, E.A., Tahira, A., Thamraa, A., Muhammad, I., Mohammed, A.A.** Optimization of Structural, Dielectric, and Magnetic Properties of Nanocrystalline Copper doped Spinel Ferrites *Materials Science and Engineering: B* 297 2023: pp. 116739. https://doi.org/10.1016/j.mseb.2023.116739
10. **Kashif, M., Sabir, I., Mingxia, He., Anwar, H., Yizhu, Z.** Utilization of Copper doped Zinc Spinel Ferrites Nanocomposites as Battery-grade Electrode Materials for Supercapattery Device Applications *Journal of Energy Storage 112* 2025: pp. 115498. https://doi.org/10.1016/j.est.2025.115498
11. **Aamir, M., Asghari, M.** High-frequency Dielectric Response of 3d metal (Mn and Cu) doped Zinc Ferrite Nanoparticles for Microwave Applications *Materials Today Communications* 34 2023: pp. 105042. https://doi.org/10.1016/j.mtcomm.2022.105042
12. **Hussain, M., Hussain, A., Hussain, A., Abbas, S., Khan, M., Alanazi, F., Alshehri, N.** Optimizing $ZnFe_2O_4$ with Copper Substitution for Improved

Lithium Storage Performance *Inorganic Chemistry Communications* 171 2024: pp. 113572. https://doi.org/10.1016/j.inoche.2024.113572

13. Optimizing $ZnFe_2O_4$ with Copper substitution for Improved Lithium Storage Performance *Inorganic Chemistry Communications* 171 2025: pp. 113572. https://doi.org/10.1016/j.inoche.2024.113572
14. **Singh, S., Sahai, A., Katyal, S.C., Goswami, N.** Structural, Optical and Vibrational study of Zinc Copper Ferrite Nanocomposite Prepared by Exploding Wire Technique *Materials Science -Poland* 36 2018: pp. 722 – 732. https://doi.org/10.2478/msp-2018-0084
15. **Komal, Y., Gulzar, A., Chauhan, H.S.** Green Synthesis of Cu-Doped Zinc Nano Ferrite materials using Moringa Oleifera Leaves *Journal of Indian Research* 10 2022: pp. 57 – 64.
16. **Nadhiya, D., Kala, A., Sasikumar, P., Mustafa, K.A.M., Thirunavukkarasu, P., Prabhaharan, M., Karnan, C., Salim, A., Majid, S.J., Asad, S., Abdallah, M.E., Nouf, S.S.Z.** Influence of Cu^{2+} Substitution on the Structural, Optical, Magnetic, and Antibacterial behaviour of Zinc Ferrite Nanoparticles *Journal of Saudi Chemical Society* 27 2023: pp. 101696. https://doi.org/10.1016/j.jscs.2023.101696
17. **Vani, A., Ganesh, K., Lalitha, G.** Structural and Optical Properties of Copper-Doped Zinc Ferrites Using Solid State Reaction Method *Materials International* 7 2025: pp. 1 – 13. https://doi.org/10.33263/Materials71.001
18. **Bera, S., Prince, A.A.M., Velmurugan, S., Raghavan, P.S., Gopalan, R., Panneerselvam, G., Narasimhan, S.V.** Formation of Zinc Ferrite by Solid-state reaction and its Characterization by XRD and XPS *Journal of Materials Science* 36 2001: pp. 5379 – 5384. https://doi.org/10.1023/A:1012488422484
19. **Ruixin, Y., Jianhui, Z., Zhiwei, Z., Fuyi, C.** Copper Substituted Zinc ferrite with Abundant oxygen vacancies for Enhanced Ciprofloxacin Degradation via Peroxymonosulfate Activation *Journal of Hazardous Materials* 390 2020: pp. 121998. https://doi.org/10.1016/j.jhazmat.2019.121998
20. **Yenchun, L., Jarnchih, H., Yenpei, F., Kuoan, T.** Preparation of Cu–Zn Ferrite Photocatalyst and it's Application *International Journal of Hydrogen Energy* 41 2016: pp. 15696 – 15702. https://doi.org/10.1016/j.ijhydene.2016.04.127
21. **Tony Dhiwahar, A., Sundararajan, M., Sakthivel, P., Chandra Sekhar, D., Yuvaraj, S.** Microwave-assisted Combustion Synthesis of Pure and Zinc-Doped Copper Ferrite Nanoparticles: Structural, Morphological, Optical, Vibrational, and Magnetic Behaviour *Journal of Physics and Chemistry of Solids* 138 2020: pp. 109257. https://doi.org/10.1016/j.jpcs.2019.109257
22. **Sundararajan, M., Sukumar, M., Dash, C.S., Sutha, A., Suresh, S., Ubaidullah, M., Al-Enizi, A.M., Raza, M.K., Kumar, D.** A Comparative study on $NiFe_2O_4$ and $ZnFe_2O_4$ Spinel Nanoparticles: Structural, Surface Chemistry, Optical, Morphology and Magnetic Studies *Physica B: Condensed Matter* 644 2022: pp. 414232. https://doi.org/10.1016/j.physb.2022.414232
23. **Charles Prabakar, A., Sathyaseelan, B., Killivalavan, G., Iruson, B., Senthilnathan, K., Manikandan, E., Sivakumar, D.** Photocatalytic dye Degradation Properties of Zinc Copper Ferrites Nanoparticles *Journal of Nanostructures* 9 2019: pp. 694 – 701. https://doi.org/10.22052/JNS.2019.04.011
24. **Shwetambaram Anuj, J., Vakil, Z.** Synthesis of Zinc-Copper Nano-Ferrite and Characterization of Their Structural, Electrical and Magnetic Behaviours *International Journal of Chem Tech Research* 6 2014: pp. 2207 – 2209.
25. **Maria Angelin Sinthiya, M., Ramamurthi, K., Mathuri, S., Manimozhi, T., Kumaresan, N., Mahesh, M., Karthika, P.C.** Synthesis of Zinc Ferrite ($ZnFe_2O_4$) Nanoparticles with Different Capping Agents *International Journal of Chem Tech Research* 7 2014 2015: pp. 2144 – 2149.
26. **Devi, E.C., Singh, S.D.** Manifestation of Magnetic Characteristics of Zinc Ferrite Nanoparticles Using the Langevin Function *Journal of Superconductivity and Novel Magnetism* 34 2021: pp. 617 – 622. https://doi.org/10.1007/s10948-020-05732-7
27. **Bayan, E., Mokliak, M., Rusalev, Y., Tolstunov, M.** Effect of Fuel type and Synthesis Temperature on Magnetic Properties of $ZnFe_2O_4$ Nanomaterials Synthesized by Sol-gel Method *Journal of Sol-Gel Science and Technology* 111 2024: pp. 783 – 793. https://doi.org/10.1007/s10971-024-06489-4
28. **Kanak Parmar, S.P., Jeong Hun, K., Amita, B., Piyush, D., Pawan, K.T., Phuruangrat, A., Lee, J.S.** Superparamagnetic and Perfect-Paramagnetic Zinc Ferrite Quantum Dots from Microwave-Assisted Tunable Synthesis *ACS Omega* 7 2022: pp. 31607 – 31611. https://doi.org/10.1021/acsomega.2c04668
29. **Maria, K.H., Choudhury, S., Hakim, M.A.** Structural Phase Transformation and Hysteresis Behaviour of Cu-Zn Ferrites *International Nano Letters* 3 2013: pp. 1 – 10. https://doi.org/10.1186/2228-5326-3-42
30. **Wahid, S.S., Abdul, H.M., Mohd, R.H., Mohd, K.Z.M., Holilah, D.P., Hasliza, B.** Cu doped $ZnFe_2O_4$ Photocatalysts for Enhanced Hydrogen Production and Dye Degradation in the Visible Region *Journal of Photochemistry and Photobiology A: Chemistry* 453 2024: pp. 115658. https://doi.org/10.1016/j.jphotochem.2024.115658
31. **Hadi, M., Batoo, K.M., Chauhan, A., Aldossary, O.M., Verma, R., Yang, Y.** Tuning of Structural, Dielectric, and Electronic Properties of Cu Doped Co–Zn Ferrite Nanoparticles for Multilayer Inductor Chip Applications *Magnetochemistry* 7 2021: pp. 53. https://doi.org/10.3390/magnetochemistry7040053
32. **Kanagesan, S., Hashim, M., AB Aziz, S., Ismail, I., Tamilselvan, S., Alitheen, N.B., Swamy, M.K., Purna Chandra Rao, B.** Evaluation of Antioxidant and Cytotoxicity Activities of Copper Ferrite ($CuFe_2O_4$) and Zinc Ferrite ($ZnFe_2O_4$) Nanoparticles Synthesized by Sol-Gel Self-Combustion Method *Applied Science* 6 2016: pp. 184. https://doi.org/10.3390/app609018

© Ge et al. *2026* Open Access This article is distributed under the terms of the Creative Commons Attribution 4.0 International License (http://creativecommons.org/licenses/by/4.0/), which permits unrestricted use, distribution, and reproduction in any medium, provided you give appropriate credit to the original author(s) and the source, provide a link to the Creative Commons license, and indicate if changes were made.